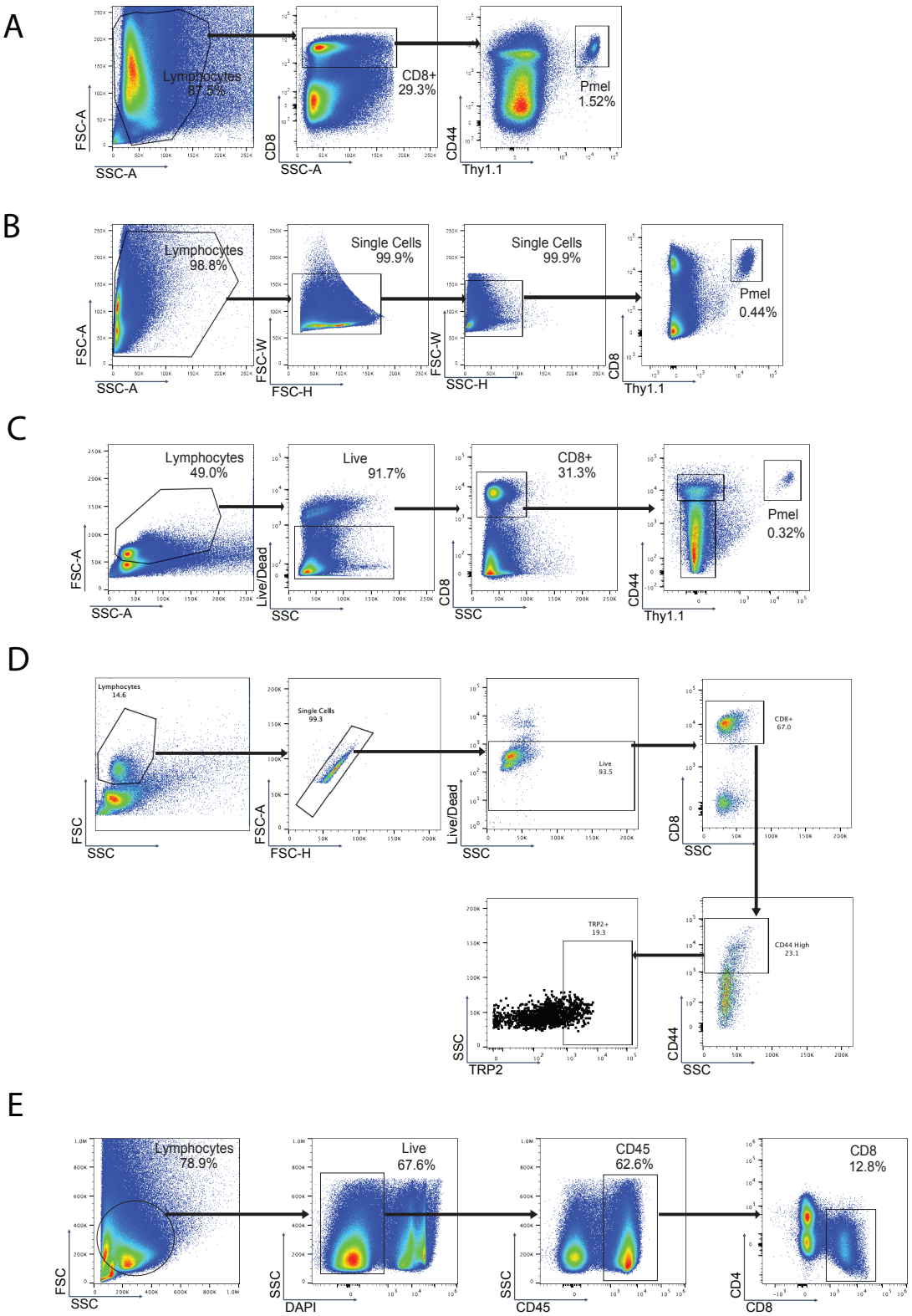

Figure S1. Flow cytometry and FACS gating strategies, Related to STAR Methods. (A) Gating for flow cytometry analyses shown in Figures 1 and 2. (B) Gating for pmel cell FACS sorting for RNAseq and scRNAseq shown in Figures 1 and 3. (C) Gating for characterization of LN T_{RM} shown in Figure 4. (D) Gating for tetramer staining and phenotyping shown in Figure 5. (E) Gating for CD8 T cell sorting of human T cells for scRNA-seq shown in Figure 7.

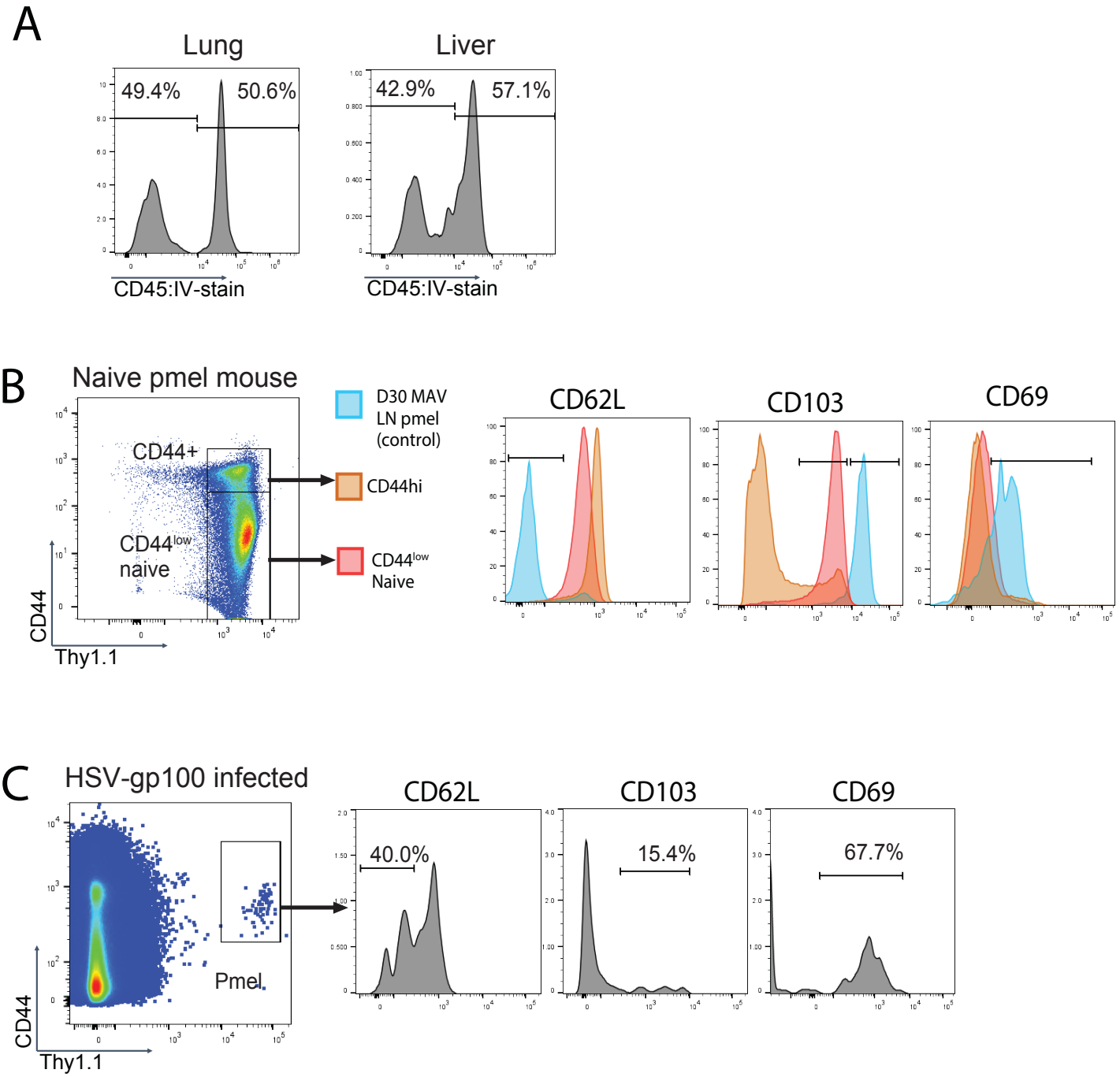

Figure S2. Staining controls for pmel populations, Related to Figure 1. (A) Mice with MAV underwent *in vivo,* intravenous staining with anti-CD45 mAb, to differentiate parenchymal vs. perivascular pmel subpopulations in lungs and liver. Histograms are gated on live, $CD8^{+}Thy1.1^{+}$ pmel cells in perfused tissue (stained populations are considered perivascular). Data are representative of two experiments each involving n=5 mice. (B) T cells from a naïve pmel mouse were phenotyped; dot plot is gated on live $CD8^{+}$ cells from inguinal LNs. Phenotypes of $CD44^{hi}$ (orange) and $CD44^{lo}$ (red) pmel subsets are shown relative to that of Trm pmel cells from inguinal LNs of a mouse with MAV (blue), for comparison. The experiment was performed twice with similar results. (C) C57BL/6 mice received 10^4 pmel cells, followed by i.p. infection with $4x10^5$ PFU HSV expressing human gp100. Inguinal LNs were harvested 30 d later and stained for $Thy1.1^{+}$ pmel cells and the indicated phenotypic markers. Representative dot plot is gated on live $CD8^{+}$ cells, and histograms are gated on $CD44^{+}Thy1.1^{+}$ pmel cells, as shown. The experiment was performed twice with similar results.

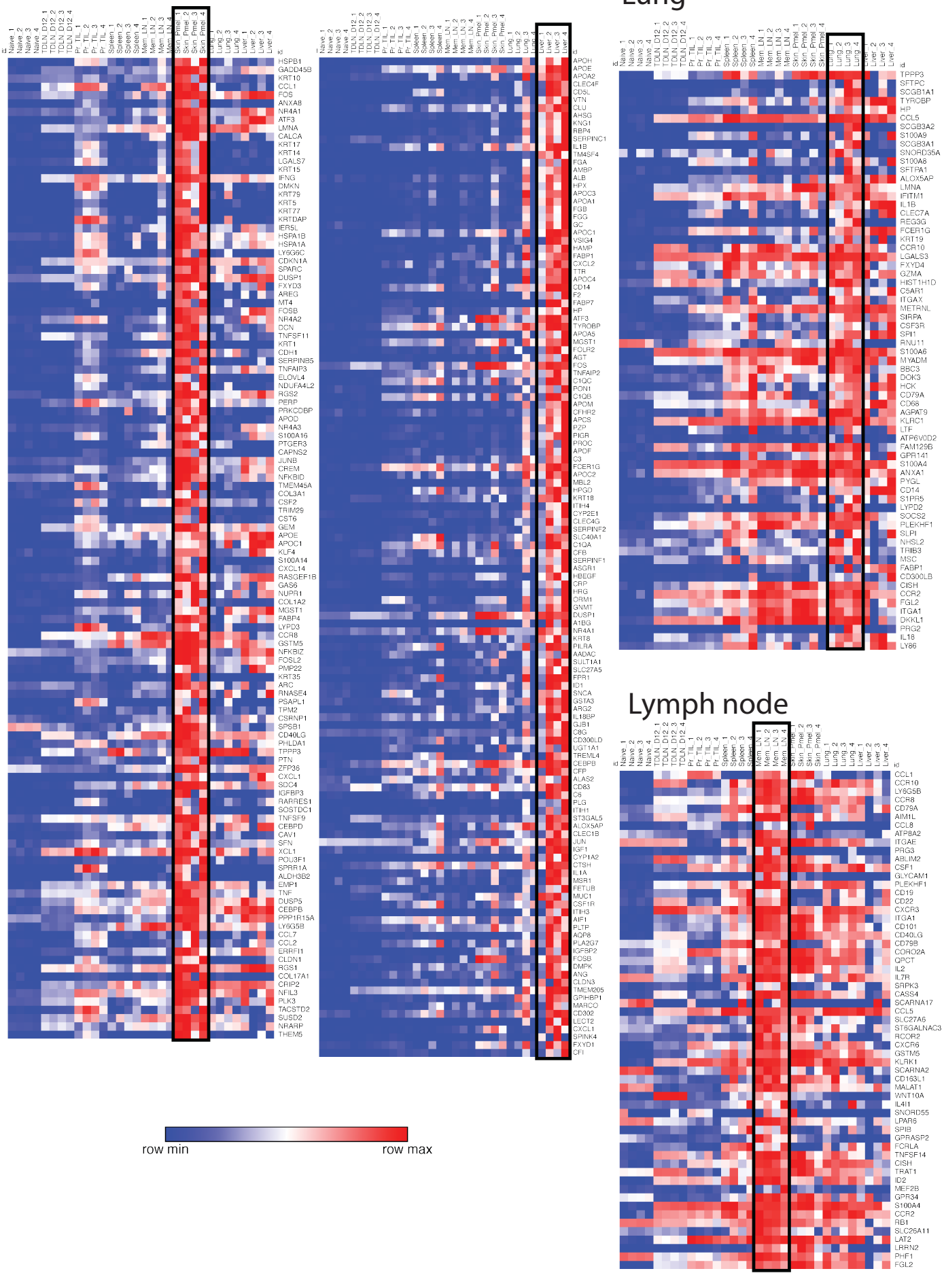
Skin
Liver
Lung
Lymph node
row min
row max

Figure S3. Tissue transcriptional signatures define tumor-specific CD8 T cells in peripheral tissues, Related to Figure 1. Mice were treated to induce MAV as in Fig. 1A. Thy1.1+ pmel cells were isolated by FACS from RLN and B16 tumors on day 12 (the day of tumor excision), and then from RLN, spleen, skin, lung, liver 45 days post-surgery. Gene expression was determined from FAC-sorted pmel cells (pooled from 5 mice/sample) by single end 75 bp full length poly-A RNA-sequencing, as described in schematic diagram in Figure 2A. Quadruplicate samples were analyzed from each tissue site, as indicated on the top of each row. Genes with a weight of 0.3 and higher (in each tissue relative to other tissues; see STAR Methods) were determined to be tissue specific and are shown above. Heatmaps were generated using browser-based software, Morpheus.

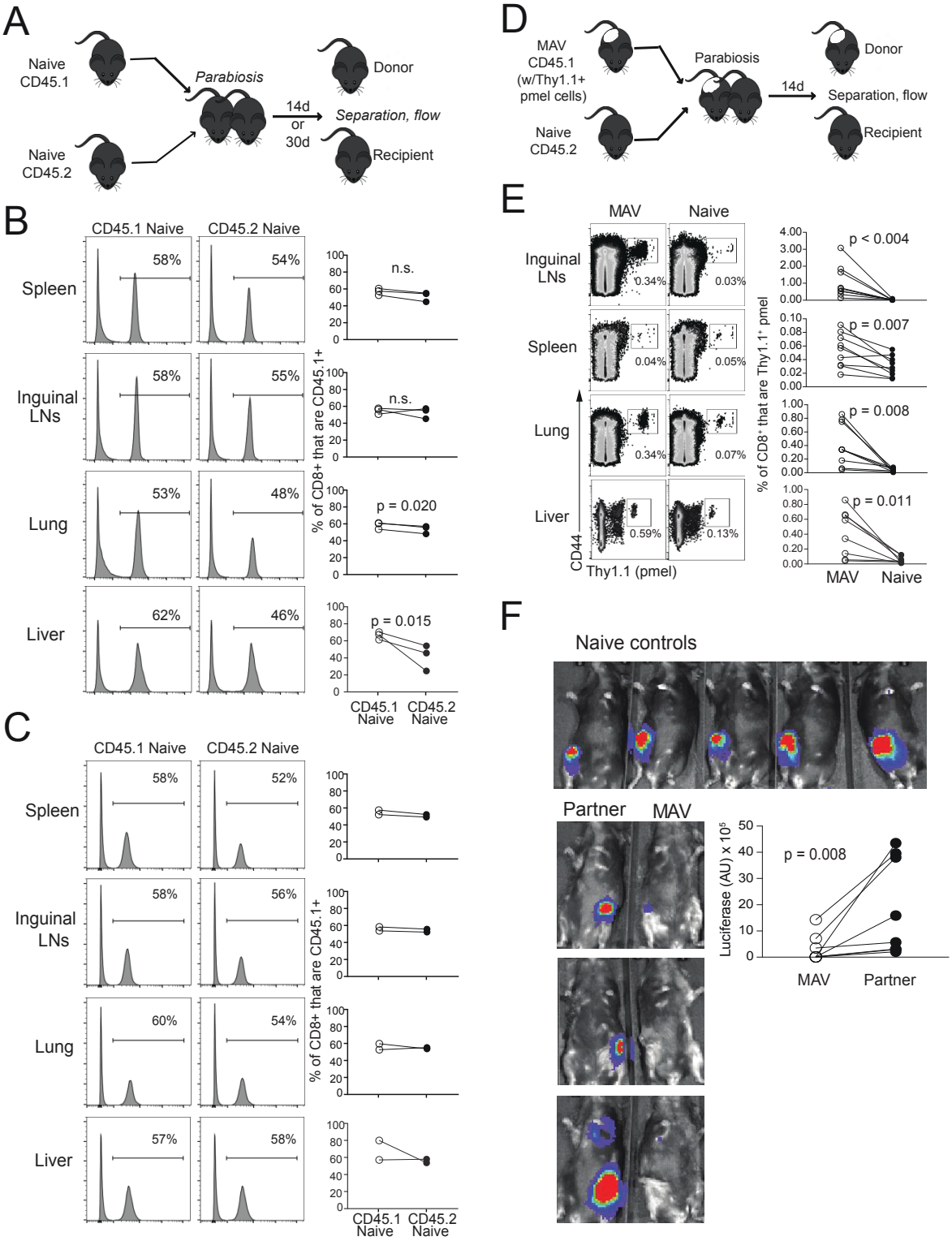

Figure S4. Parabiosis immune equilibration controls, Related to Figures 2 and 6. (A) Experimental schematic depicting the parabiosis surgery with naïve CD45.1 and CD45.2 C56BL/6 mice. Percent of $CD8^+CD45.1^+$ cells was assessed in indicated tissues gated on $CD8^+$ cells either (B) 14 days or (C) 30 days post parabiotic surgery. (D) Experimental schematic depicting the parabiosis surgery for testing tumor-specific CD8 T cell residency with naïve recipient mice. (E) Distribution of $Thy1.1^+$ pmel cells (gated on $CD8^+$) in indicated tissues. (F) Mice were treated as in Figure 6H and rechallenged with $5x10^4$ B16-luciferace cells injected directly into regional LNs (RLN); LN tumor burden was imaged 7 days later. Symbols represent individual mice, with lines joining parabiotic partners. Significance was determined by paired *t* test or Wilcoxon matched pairs test; non-significant (n.s.) indicates $p > 0.05$. Data shown are from a single experiment (B and C), or pooled from two independent experiments (E and F).

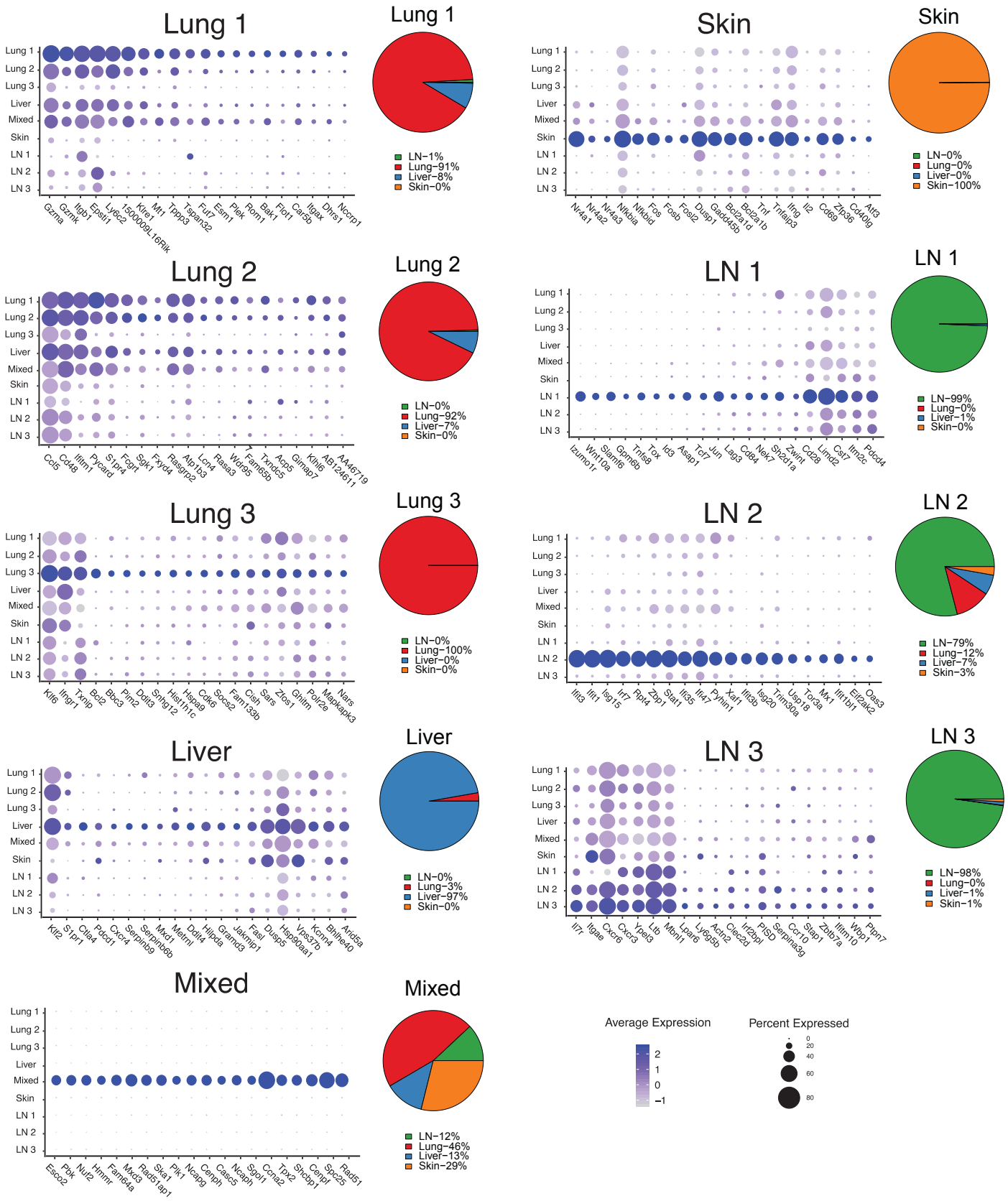

Figure S5. Pmel T cell heterogeneity within each tissue is defined by unique gene expression patterns, Related to Figure 3. As described in Figure 3, FAC-sorted pmel T cells underwent 3'-end single cell RNA-seq using the 10x Genomics platform. For each cluster in Figure 3, gene signatures comprised of the most significantly upregulated genes were defined by the *FindMarkers* build-in function in Seurat. Dot plots depict average Z-transformed normalized expression of the top 20 representative genes in each cluster. Pie charts depict the percentage of cells from each tissue that comprise each cluster.

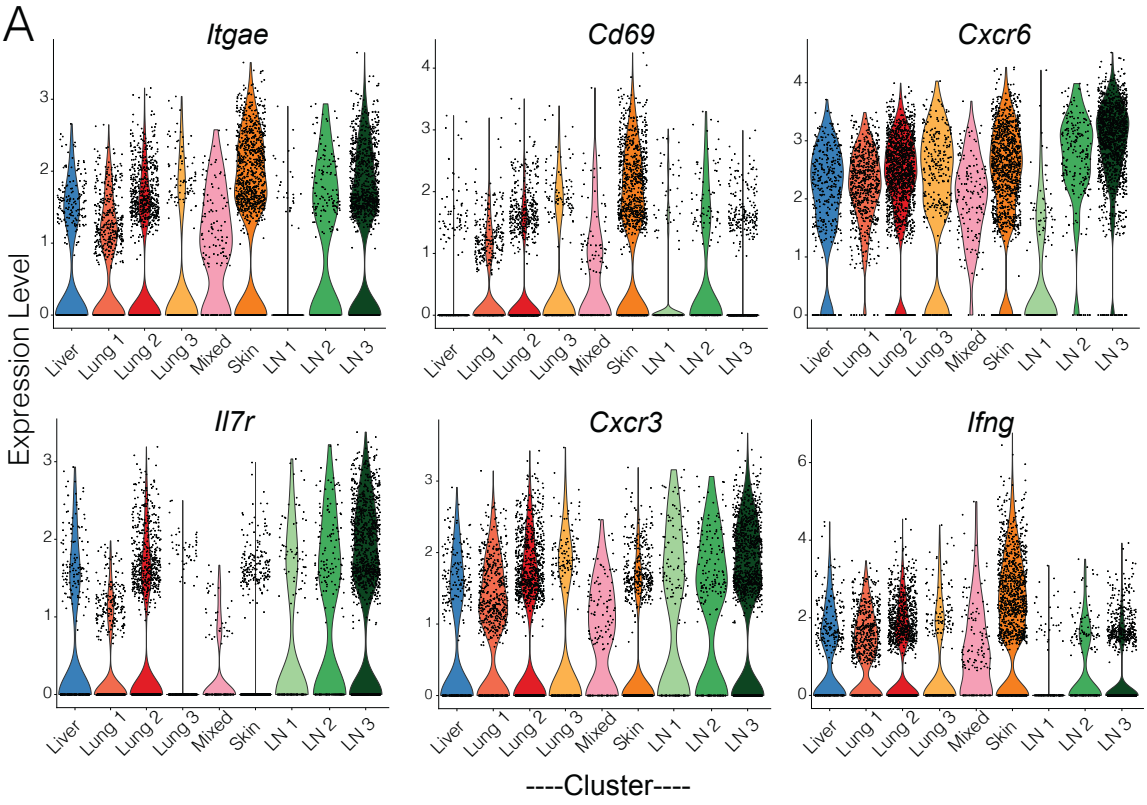

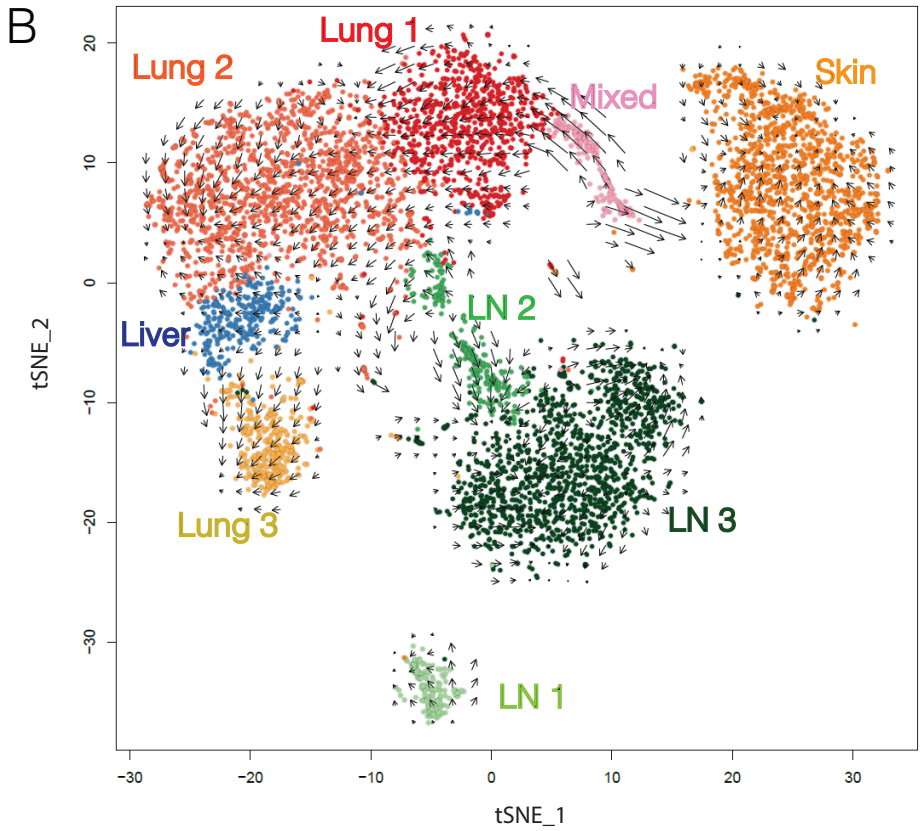

Figure S6. Gene expression and RNA velocity analyses of single cell RNAseq data, Related to Figure 3. (A) Violin plots depicting average Z-transformed normalized expression of select T_{RM} markers across clusters shown in Figure 3. (B) RNA velocity field projection onto the t-SNE plot of memory T cells shown in in Figure 3. Each dot corresponds to a single cell; arrows depict the local average velocity. Clustering was done using "pagoda2" with velocity estimations determined with "velocyto.R" R packages..

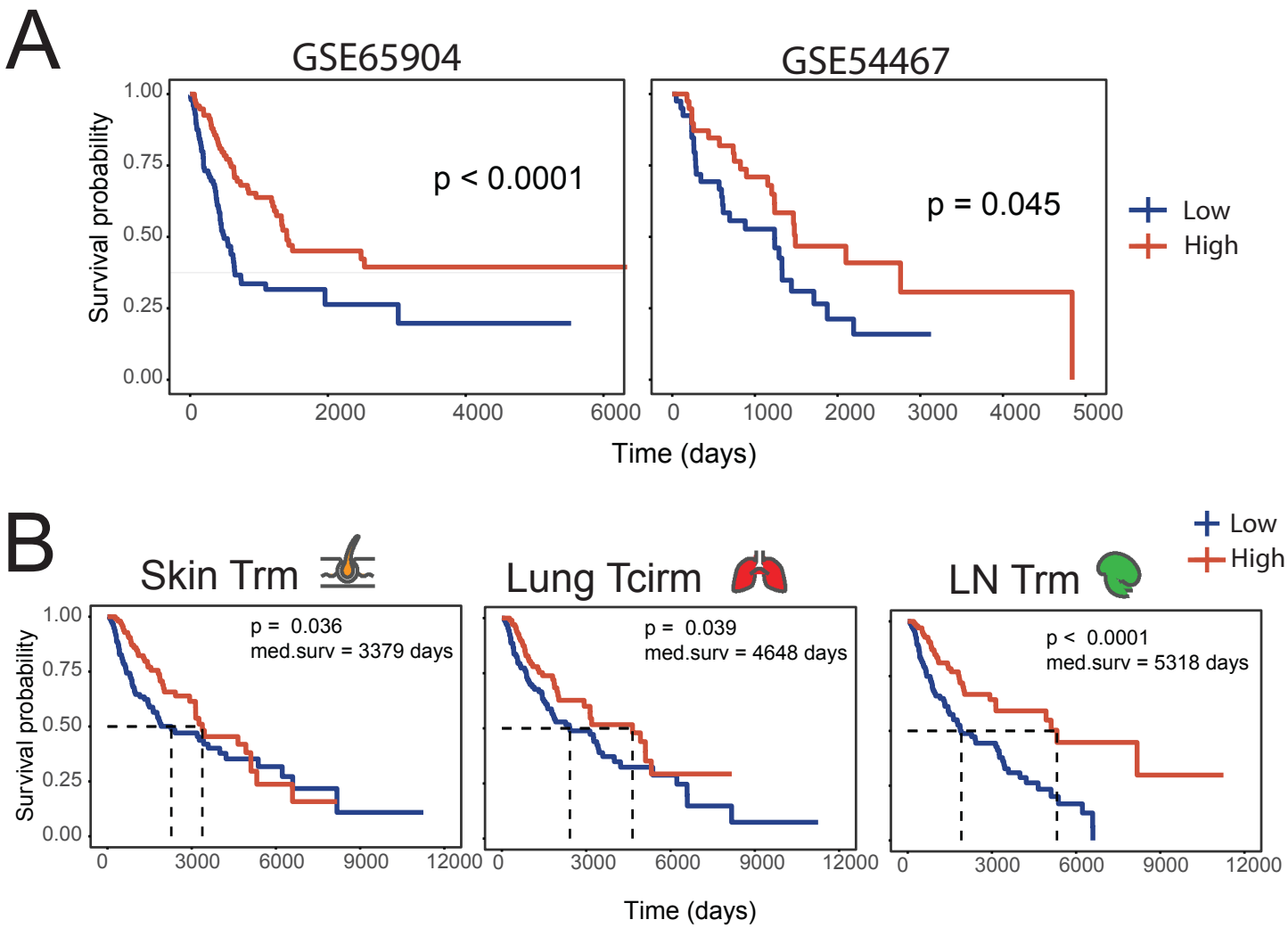

Figure S7. The lymph node T_{RM} gene signature is prognostic in patients with metastatic melanoma, Related to Figure 7. The LN T_{RM} gene signature was generated as described in Figure 7G. (A) Kaplan-Meier plots indicating the prognostic value of stratification based on enrichment of single cell-derived binary LN Trm T cell signatures in regional lymph node metastases for public datasets GSE53118 containing 79 patients, and GSE65904 containing 195 patients. (B) Survival analyses were conducted using TCGA regional LN metastatic specimens, as described in Figure 7H, but with CD8 T cell specific genes (*Cd8a, Cd8b1, Cd3g, Cd3e,* and *Trav7-4*) not added to the signatures. In all analyses, patients were divided into high vs. low enrichment groups based on separation at the median.

Table S1, Related to Figure 3: Comparison of marker expression on pmel cells across methods and tissues

Tissue	Method	CD103/*Itgae*	CD62L/*Sell*	CD69	CXCR6	CD127	CXCR3
Lymph Node	Protein (Flow)	High	Low	High	Very High	High	High
	Bulk RNA	High	Low	Intermed	Very High	High	HIgh
	scRNA	High	Absent	Intermed	Very High	High	High
Skin	Protein (Flow)	Very High	Absent	Very High			
	Bulk RNA	High	Absent	High			
	scRNA	High	Absent	High			
Lung	Protein (Flow)	Intermed	Low	Intermed			
	Bulk RNA	High	Low	Intermed			
	scRNA	Intermed	Absent	Intermed			
Liver	Protein (Flow)	Intermed	Low	Intermed			
	Bulk RNA	Intermed	Low	Intermed			
	scRNA	Intermed	Absent	Intermed			
Spleen	Protein (Flow)	Intermed	Low	Intermed			
	Bulk RNA	Intermed	Intermed	Low			
Naïve	Protein (Flow)	Intermed	High	Low			
	Bulk RNA	Intermed	High	Low			

Protein expression not assessed

Expression levels (Very High, High, Intermediate, Low, Absent) are described relative to the following pmel control populations:

	Positive	**Negative**
Flow cytometry	Skin	Naïve
Bulk RNA	Skin	Naïve & TILs
scRNA	Skin	None

Supplemental Table 2, Related to Figure 7: Tissue specific transcriptional signatures

Skin_Trm				Lung_Circm				LN_Trm	
ACTB	EMD	JUND	RGS2	ABRACL	ESD	PDLIM1	S100A10	ACAP1	LY6G5B
AKAP13	ENO1	KDM6B	RHEB	ACTG1	ESM1	PDLIM2	S100A11	ACTN2	MALAT1
ALDOA	ERDR1	KLF10	RORA	AIMP1	FLOT1	PGLYRP1	S100A4	AMICA1	MBNL1
ANXA1	ETS1	KLF6	RPL15	ANXA2	FUT7	PHF5A	S100A6	ARHGEF1	MRPL52
ANXA2	FASL	LCP1	RPL35	ANXA6	GAPDH	PKP3	S1PR4	ATXN7L3B	MXD4
ARID5A	FGL2	LDHA	RRAD	AP2S1	GGT1	PLEK	SEC61B	AW112010	MYCBP2
ATF3	FKBP2	LITAF	RSRC2	APRT	GIMAP1	PLP2	SERPINB6A	B4GALNT1	N4BP2L2
ATP2B1	FOS	LMNA	SAMSN1	ARL6IP5	GIMAP7	POLR1D	SERPINB6B	BCL11B	NDUFA3
AY036118	FOSB	LRRC58	SAP18	ARPC1B	GLIPR2	PPP1CA	SH2D1A	CBX3	NDUFA5
B4GALT1	FOSL2	LY6G5B	SAT1	ARPC3	GLRX	PRDX1	SIKE1	CCND2	NKTR
BHLHE40	FTH1	MALAT1	SERTAD1	ARPC5	GLTSCR2	PRELID1	SNRPE	CCR10	NUDCD3
BRD2	FTL1	MIF	SIT1	ATP1B3	GLUD1	PRR13	SRP19	CD27	OGT
BTG1	FUS	MXD4	SLBP	ATP5C1	GM2A	PSMB4	SSR3	CD7	PDCD4
BTG2	GADD45B	MYH9	SLC38A2	ATP5F1	GMFG	PSMD8	SURF1	CD74	PDIA3
CALM1	GAPDH	NDFIP1	SLC3A2	BAK1	GNA15	PSME1	TAGLN2	CHD3	PDIA6
CALM2	GCH1	NEURL3	SMAD7	BC021614	GNB2L1	PYCARD	TKTL1	CIRBP	PTPN7
CAPG	GEM	NFKBIA	SMCO4	BSCL2	GZMA	PYHIN1	TMSB4X	CLEC2D	PTPRC
CAPNS1	GM6133	NFKBID	SOCS1	BTF3	GZMB	RAC2	TOMM22	CROT	RAPGEF6
CCDC107	GNB1	NFKBIZ	SQSTM1	CAR5B	GZMK	RACGAP1	TPPP3	CSF1	RBPJ
CCL4	GPR132	NR3C1	SRSF2	CARHSP1	HMGB2	RASA3	TSPAN32	CXCR3	RGS10
CCND2	GSTP1	NR4A1	STK17B	CCDC12	ICT1	RASGRP2	TWF2	CXCR6	RPL15
CD28	H3F3B	NR4A2	TAGAP	CCL5	IFITM1	RBM3	TXN1	EIF5	RPL35
CD40LG	HERPUD1	NR4A3	TBX21	CCR2	IFITM2	REEP5	TXNDC5	EVL	RPL38
CD44	HILPDA	ODC1	TESC	CCT2	IFITM3	RILPL2	UQCRFS1	FAM189B	RPS28
CD6	HIVEP2	ORAI1	TGFB1	CD47	IGBP1	RNH1	VIM	FUBP1	RPS29
CD69	HMGN1	PDCD1	TGIF1	CD48	ITGAX	ROM1	WDR95	FYB	SASH3
CD82	HSD11B1	PDIA3	THY1	CDC25B	ITGB1	RPL10		GRAMD1A	SEMA4A
CDKN1A	HSP90AB1	PDIA6	TMEM123	CDC42	KLHL6	RPL10A		GSTP1	SHISA5
CHD4	HSP90B1	PFN1	TMEM256	CLIC1	KLRD1	RPL22		H2-T23	SIPA1
CISH	HSPA5	PHLDA1	TNFAIP3	CLTA	KLRE1	RPL24		HMGN1	SLFN2
CITED2	HSPA8	PIM1	TNFAIP8	CMTM7	KXD1	RPL28		HMHA1	SP100
CLK1	ICAM1	PKM	TOB1	CORO1A	LAT2	RPL29		HSP90B1	SPCS2
COQ10B	ICOS	PLD3	TOMM6	CORO1B	LGALS1	RPL31		ID2	SRRM2
COTL1	IER2	PNRC1	TUBA4A	COX4I1	LGALS3	RPL39		IFITM10	STAP1
CREM	IER5	POLR2L	UBA52	COX5B	LGALS3BP	RPL4		IKZF3	TBC1D10C
CSRNP1	IFNAR1	PPP1R11	UBC	CRIP1	LSP1	RPL7		IL16	TESC
CTLA2A	IFNG	PPP1R15A	UBE2S	CSNK2B	MRPL30	RPL7A		IL18R1	TNFAIP8
CTSW	IFNGR1	PPP1R16B	USMG5	CTLA2B	MRPS16	RPLP0		IL7R	TNRC6A
D16ERTD472E	IFRD1	PRDX6	USP50	DAP	MS4A6B	RPS10		IRF2BPL	TSC22D4
DNAJA1	IL2	PRKAR1A	VGLL4	DHRS1	MSRB1	RPS11		ITGAE	UBA52
DNAJB1	IL21R	PRR7	VPS37B	EBP	MT1	RPS12		ITGAL	UCP2
DUSP1	IL2RB	PTMA	WBP1	EEF1B2	MYL6	RPS17		ITM2C	WBP1
DUSP5	IL2RG	PTP4A1	WNK1	EEF2	MYO1G	RPS2		LFNG	XIST
DYNLL1	ITGAE	PTPN22	WSB1	EIF3F	NACA	RPS20		LPAR6	YPEL3
EIF1	ITK	QPCT	YBX1	EIF3H	NCCRP1	RPS26		LRRC58	ZBTB7A
EIF4A1	ITM2B	RAPGEF6	YWHAZ	EIF3I	NPC2	RPS27L		LTB	ZNRF1
EIF5A	ITPKB	RGCC	ZC3H12A	EIF4E2	NRP1	RPS4X		LY6A	
EMC10	JUNB	RGS1	ZFP36	EPSTI1	NUDT21	RPSA		LY6E	
			ZFP36L1						
			ZFP36L2						
			ZNRF1						

Supplemental Table 3, Related to Figure 7: Patient Characteristics

Patient study identifier	Age	Sex	Treatment	Lymph node metastasis type	Tumor size in LN	Experiment	Data shown in
sd-07-12291B2	58	M	Surgery	sentinel	4.6mm	IHC	Fig. 7A
sd-08-11049F1	57	F	Surgery	sentinel	2.6mm	IHC	not shown
sd-09-24757B1	54	F	Surgery	sentinel	2.9mm	IHC	not snown
sd-08-26200C1	56	M	Surgery	sentinel	2.2mm	IHC	not shown
D16002-652	87	F	11 cycles of pembrolizumab followed by surgery	regional to abdominal oligometastatic lesion	grossly positive	Immunofluorescence	Fig. 7B
D16002-649	72	M	2 cycles of pembrolizumab followed by surgery	regional to lung oligometastatic lesion	grossly positive	single cell RNA/TCR-seq (Figure 7C-F) and Immunofluorescence	Fig. 7C-F